〈論文〉 4-4-10

# 부분 공진형 소프트 스위칭 PWM DC-DC 고전압 컨버터

김 용 주, 신 대 철

# Soft-Switched PWM DC-DC High-Power Converter with Quasi Resonant-Poles and Parasitic Reactive Resonant Components of High-Voltage Transformer

Yong-Ju Kim and Dae-Chul Shin

## ABSTRACT

This paper deals with a fixed frequency full-bridge inverter type DC-DC high-power converter with high frequency high voltage(HFHV) transformer-coupled stage, which operates under quasi-resonant ZVS transition principle in spite of a wide PWM-based voltage regulation processing and largely-changed load conditions. This multi-resonant(MR) converter topology is composed of a series capacitor-connected parallel resonant tank which makes the most of parasitic circuit reactive components of HFHV transformer and two additional quasi-resonant pole circuits incorporated into the bridge legs. The soft-switching operation and practical efficacy of this new converter circuit using the latest IGBTs are actually ascertained through 50kW-120kV trially-produced converter system operating using 20kHz/30kHz high voltage(HV) transformers which is applied for driving the diagnostic HV X-ray tube load in medical equipments. It is proved from a practical point of view that the switching losses of IGBTs and their electrical dynamic stresses relating to EMI noise can be considerably reduced under a high frequency(HF) switching-based phase-shift PWM control process for a wide load setting requirements.

**Key Words**: Resonant-Ploe, Zero Voltage Switching, High Voltage Transformer, Soft-Switching, X-ray

## 1. Introduction

In recent years, the modern practical developments of soft-switching transition mode inverter-fed DC-DC high-power converter circuits using new MOS gate-derived semiconductor devices/modules with intelligent drive circuits have attracted special interest from a practical point of view, regarding efficient and high-performance HF switching-based PWM and PFM/PDM DC-DC converter topologies operating under the principles of ZVS, ZCS and ZVS-ZCS hybrid commutation modes.

As compared with commonly-used hard- switching DC/DC power converters with HF link, the new family of soft-switching power conversion circuit technologies which incorporates resonant-switches, resonant DC link, resonant AC link and resonant-poles into the conventional power conversion circuit structures have begun to be investigated in order to minimize the switching losses under HF switching-modulated operation of MOS-gate power semiconductor devices, their electrical transient-stresses without snubber circuits and the related noise generation problems.

With a rapid progress of multi-diverse new power semiconductor devices such as application-specific IGBTs, MCTs and B-SI transistors, and their related optimum drive circuit interfaces, the soft-switching high-power conversion circuits with a HF isolated link

and their control strategies have been developed for low-noise, high-power density power supplies required from a practical standpoint.[1~2]

Of some resonant mode circuit topologies, the auxiliary basic resonant commutation pole topology and its extended versions incorporated into two bridge legs are more suitable and acceptable for application specific high-power converter applications.

Under these technological backgrounds, the high-performance, lowered electromagnetic noise, compact multi-resonant ZVS-PWM inverter-fed DC-DC converter using IGBTs for new diagnostic X-ray HV power generator have been developed as general and gastrointestinal radiology.[3~5]

This paper presents a novel prototype of resonant pole-assisted zero voltage soft-switching phase-shift PWM DC-DC high-power converter with HFHV transformers-link.

This converter circuit modeling is exactly introduced including parasitic circuit parameters as resonant elements of HFHV transformers and DC feeding cable as smoothing filter element in series with X-ray tube load expressed by a variable resistance circuit.

Its operating characteristics in steady-state are effectively illustrated on the basis of computer-aided simulation analysis.

A trially-produced resonant pole-assisted 50kW-120kV multi-resonant PWM DC-DC converter making the most of internal parasitic LC resonant circuit components which are included into the two 20kHz HV transformers with a large turn-ratio; 1: 500, and the input capacitance of HV DC cable is evaluated from an experimental point of view.[6]

## 2. Series-Capacitor Connected Transformer Parallel Resonant DC-DC Converter

Fig. 1 shows a schematic previously-proposed power conversion system developed for a X-ray high-voltage power generator which incorporates a series-connected parallel hybrid resonant phase-shift PWM inverter-fed DC-DC converter using IGBTs.

This power conditioning converter system is schematically composed of a phase-controlled AC/DC converter, a full-bridge type PWM series and parallel resonant inverter-fed DC-DC converter with high-frequency HV transformer-coupled stage, a HVHF diode rectifier modules, a HV DC cable supplied into the X-ray tube load for medical power installation.

In addition to these, a resonant ZCS PFM DC-DC converter with a HF transformer link is used practically for improving a filament current regulation and EMI noise characteristics.

The total control system with the software-controlled DSP voltage and current sensor and their interfaces are incorporated into this converter in order to linearize total the converter characteristics and instantaneous input drooping voltage and ripple voltage disturbance

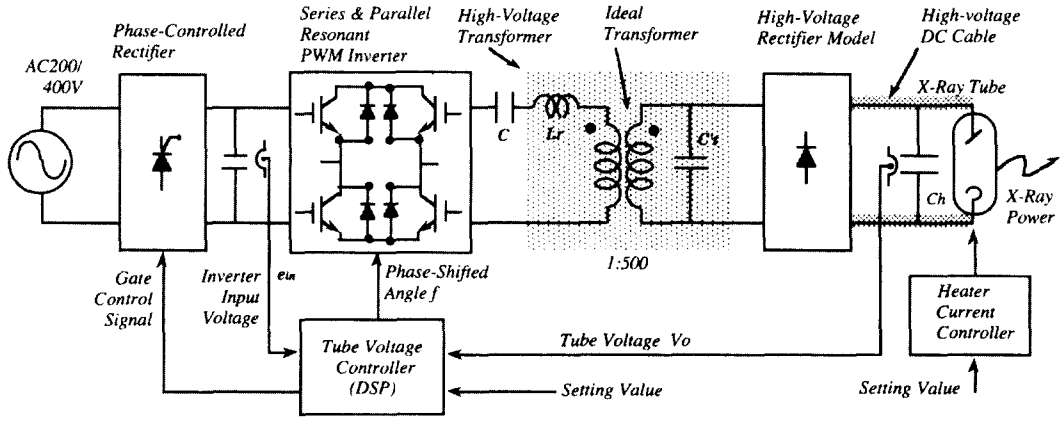


Fig. 1 Series Capacitor-connected Parallel Resonant Tank Phase-Shifted PWM DC-DC Converter with a HV Transformer Link for a Diagnostis X-ray Power Generator

cancellation, and to stabilize the X-ray tube voltage with a low fluctuating ripple X-ray radiated high-frequency power is largely concerned with a heater current ripple supplied by the regulated converter.

In this case, the equivalent electrical circuit load between anode and cathode of X-ray tube can be expressed as an adjustable varying resistance model, of which is to be varied continuously in accordance with the filament heater current settings. In a main power conversion stage, the voltage-clamped snubber circuits to absorb a spike surge voltage are practically inserted in parallel with two full-bridge inverter arms.

This phase-shifted PWM converter DC-DC converter with a series connected parallel resonant tank is characterized in terms of making the most of the following circuit parameters;

(a) The lumped parasitic leakage-inductances and lumped capacitances between secondary windings of HFHV transformer with a large high turn-ratio are used as the parallel resonant LC components.

(b) The equivalent internal capacitance observed in the input side of a high voltage DC cable is used as a DC smoothing capacitor under HV switched-mode operation.

(c) A constant HF phase-shifted PWM control strategy is introduced in combination with a phase-controlled strategy of single-phase/three-phase AC/DC converter with boost DC-DC converter or active power converter with line current sine wave shaping and unity-power factor correction.

(d) A series resonant-compensated capacitor connected in series with the primary winding of HV transformer is additionally inserted in order to stabilize the output voltage supplied to the X-ray tube in spite of largely-changed load variations and phase-shifted PWM control processing.

(e) The load resistance can be continuously varied according to adjusting a filament current of X-ray tube, which is provided through the latest ultra-high frequency quasi-resonant ZCS-PWM converter using new intelligent power devices.

(f) The X-ray tube voltage regulation system is feasibly operated under the advanced digital feedback and feed-forward control-based DSP schemes in order to improve the output voltage response characteristics when started and to increase voltage-ripple stabilization even in steady-states.

However, the practical problems to be solved for this sort of series and parallel resonant PWM DC-DC power converter with a fixed frequency phase-shifted PWM scheme especially occupies large switching losses at turn-off and snubber circuit losses when operated at a HF switching range more than 20kHz, severe surge voltage and current spike generation due to high di/dt and dv/dt values in addition to the significant increase of HF EMI/RFI noise levels.

Some types of soft-switching DC/DC power converter configurations which incorporate the quasi-resonant circuits such as resonant switch, resonant AC link, resonant DC link and resonant commutated pole topologies are feasibly considered in order to minimize the switching losses of IGBTs, their electrical stresses and noise for largely-changed load variations in PWM regulation processing from no load to full load.

In medical electronic equipments as general and gastrointestinal radiology, these problems mentioned above are more significant.

In particular, the HF transformer linked soft-switching PWM DC-DC power conversion circuits using IGBTs with resonant-commutated pole topologies are more suitable for high-power applications such as HV X-ray generator, auxiliary power supplies in telecommunication energy systems, auxiliary power supplies for transportation system, power processors for aerospace and conditioners and utility-interfaced decentralized DC-DC power supplies.

## 3. New Resonant Pole-assisted Multi-Resonant PWM DC-DC Converter System

Fig. 2 shows a total prototype system of a high-performance, low electromagnetic noise, compact DC-DC high-power converter with two HV transformer-coupled stage incorporating resonant pole-assisted ZVS-PWM inverter using the next generation IGBTs.

This converter is developed for the advanced version of X-ray HV generator which is expected as one of next generation medical power apparatuses.

Lossless snubber capacitors ($C_{s1}$-$C_{s4}$) are connected in parallel with individual IGBT incorporated the voltage-

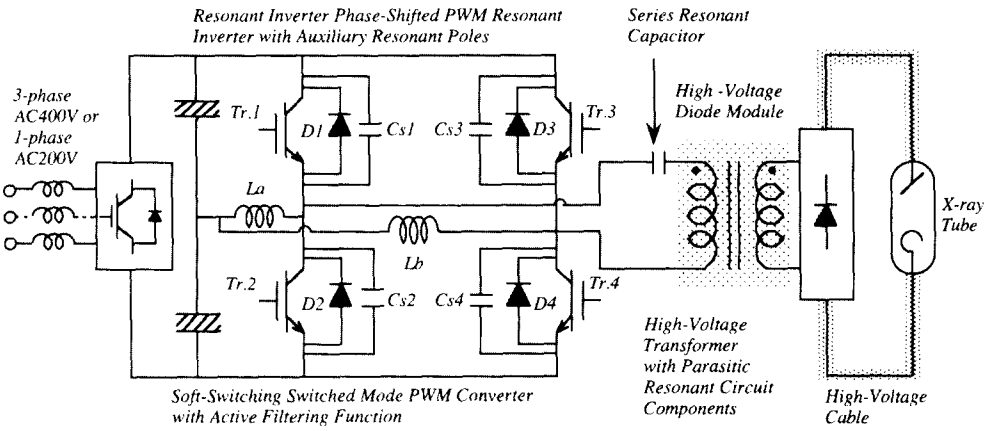


Fig. 2 Newly-developed X-ray High-Power Generator using Soft-Switching PWM Inverter Link

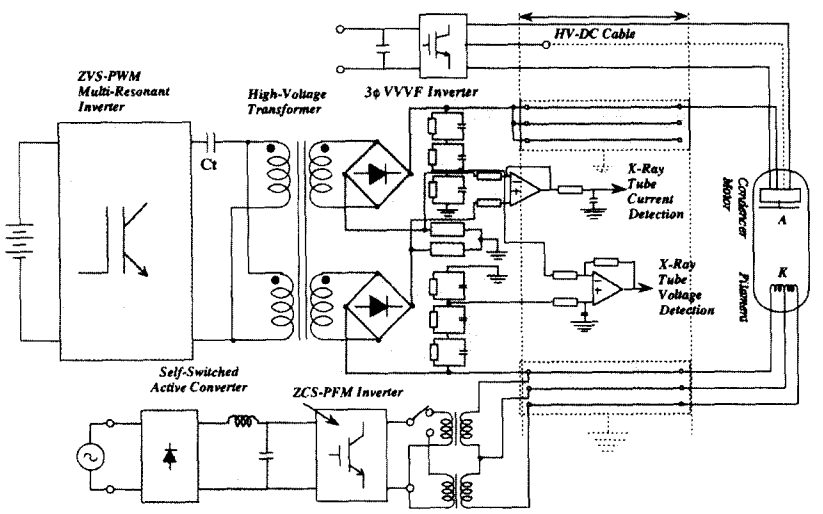


Fig. 3 Power Conversion Conditioning System Structure for High-Voltage Generator in Medical Installation X-ray

clamped snubbers into two switching bridge legs for the purpose of reducing a dynamic dv/dt and di/dt capabilities at IGBT turn-on and turn-off switching of the converter shown in Fig. 1 are preferably replaced by two resonant pole circuit, which is composed of the lossless capacitors coupled by auxiliary resonant circuits with quasi-resonant inductors, La and Lb.

Fig. 3 presents the feasible system structure in the output power converter stage of the resonant pole-assisted phase-shifting ZVS-PWM inverter. This system is composed of two HV transformers, HV DC cable supplied to the X-ray load and X-ray tube heater current regulator realized by the latest quasi-resonant ZVS converter with two HF transformers in addition to soft-switched active AC/DC converter inter link.

Fig. 4 shows the sequence chart of the switching pulse signals with a slight dead time supplied into the gate driver modules of IGBTs.

The gate voltage signals of $Q_3$ and $Q_4$ with about 50% duty-cycle are synchronously shifted with respect to the gate voltage signals of $Q_1$ and $Q_4$ with about 50% duty-cycle.

Phase-shifted angle/time $\psi(0<\psi<T/2)$ between two switching bridge arms/legs in the full-bridge circuit is

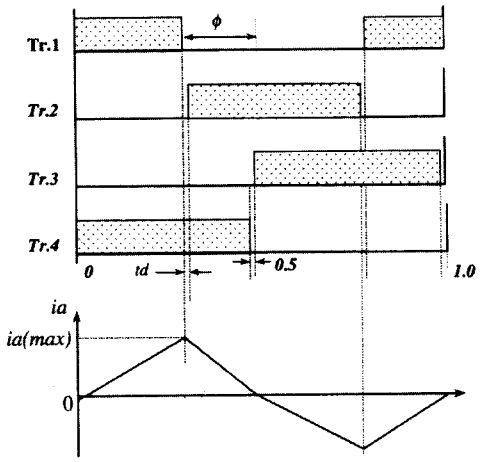


Fig. 4 The Sequence chart of Gate Switching Pulses

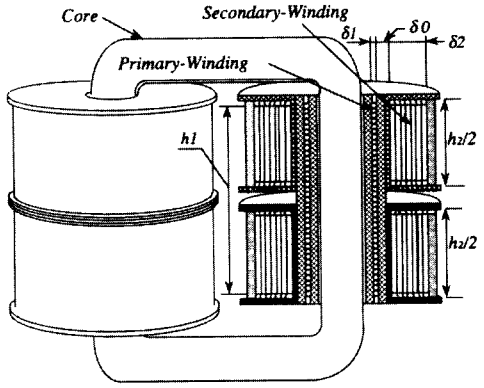


Fig. 5 High-voltage transformer for high-frequency link high-power

introduced as a control variable to regulate the output power/voltage under a constant inverter frequency setting.

In addition, the blanking time $t_d$ is an another essential specified-time in order to achieve a ZVS operation in lossless capacitor legs.

In this converter, its ZVS transition with the supply voltage-clamped restriction is based upon the charging and discharging operating principle of two lossless capacitive snubber legs with two auxiliary quasi-resonant inductor-assisted half-bridge circuits.

These include the active forward control loop to compensate the abruptly-changed DC input voltage caused by the rectifier with a low pass filter when the converter is started instantaneously and to eliminate DC input voltage disturbances with a periodic low frequency AC ripple fluctuation, linearization of nonlinear converter voltage characteristics as well as a feedback load voltage regulation loop.

## 4. HV Transformer for HF and High-Power Link and Its Design

Fig.5 shown the HV transformer suitable for high-power conditioning and processing.

The key point to the appropriate modeling lies in the method of treating leakage-inductances, the parasitic corresponding to iron and copper losses and winding capacitances of the HV transformer. The leakage inductance Lr may be approximately expressed as the lumped series inductance.

In the conventional HV transformer, the stray-capacitances exist mainly between each layer of the secondary-windings, which are isolated from one another with oil immersed paper.

The distributed stray capacitances are also treated here as a lumped stray-capacitance Cp.

Besides, the power losses of the HV transformer ought to be presented. Some of them are proportional to the square of the applied voltage and the others are determined by the current flowing through its windings.

The transformer loss is denoted by iron loss and the latter loss is specified by stray-load loss.

As discussed above, an equivalent circuit of the HV transformer is expressed in terms of a leakage inductance, the lumped stray capacitance and loss-equivalent resistances which are represented by the lumped stray-load loss and the equivalent iron loss as no-load loss.

The leakage inductance of the HV transformer is estimated as follows:

$$X_{L2} = 4\pi^2 f_{inv} N_2^2 \frac{u_1 + u_2}{2h}\left(\frac{\delta_1 + \delta_2}{3}\delta_0\right)\times 10^{-7} \cdots \quad (1)$$

$$L_{r2} = X_{12} / 2pf_{inv} \cdots \quad (2)$$

$$L_r = L_{r2} / n^2 \cdots \quad (3)$$

where, $X_{L2}$: the leakage inductance; $L_{r2}$: the secondary-side leakage inductance; $L_r$: the leakage inductance

reduced into the primary side port; finv: the inverter operating frequency; $N_2$: the turn number of the secondary windings; n; the turn ratio of the HV transformer; $u_1$ and $u_2$: the average one turn lengths of the primary and the secondary windings; $h$, $d_1$, $d_2$, and $d_0$: geometric dimensions of the HV transformer shown in Fig.3.

The lumped stray capacitance of the high voltage transformer is estimated by

$$c_p = c_{p2}n^2 = \frac{8pe_c \cdot e_0 \cdot rh_2 \cdot n^2}{3d(m-1)j^2b} \cdots \quad (4)$$

Where, $C_{p2}$: the stray capacitance of thesecondary-side windings; $C_p$: the reduced value of $C_p$ into the primary-side port; $e_0$: electric permittivity of vacuum; $e_e$: equivalent relative permittivity of the oil immersed paper; $r$: average radius of the secondary-side windings; $h_2$: the hight of the primary and the secondary winding; $d$: the distance between two layers of the secondary windings; m: the layer number of the secondary windings; $j$: the division number of the secondary windings for each leg; b:the number of the legs.

## 5. Quasi-Resonant Commutation Pole

Fig. 6 shows the idealized basic operating voltage and current waveforms of a resonant-pole circuit in the right hand side.

The circuit operation in a half-cycle stage is divided into four modes;

- Interval I; When $Q_4$ conducts at $t=t_0$, the current $i_b$ flowing through $L_b$ increases with a positive slope. $V_{c4}$ across $C_4$ becomes zero and $V_{c3}$ across $C_3$ is exactly clamped to E.
- Interval II; At the time $t=t_1$, $Q_4$ is turned off. Its current commutates to $C_3$ and $C_4$ of the lossless capacitor leg. $Vc_3$ across $C_3$ which is equal to E decreases sinusoidally until it reaches zero at the time $t=t_3$.

On the other hand, the voltage across $Q_4$ increases up to E with a mode rate slope.

- Interval III; The anti-parallel diode $D_3$ of $Q_3$ takes over the inductor current and starts conducting.
- Interval IV; $Q_3$ is turned on at the time $t=t_3$. During the conduction time of $D_3$, $Q_3$ can be turned on with no loss generation because the voltage across the power switch is zero.

The inductance current decreases with a negative slope. The polarity of the inductance voltage changes and the current increases.

In this converter, while the main power switching device is IGBT turned-off, the lossless capacitors as snubbers will enforce a low forward voltage with a limited dv/dt capability across the power switching device.

Note that each power switch turns off in lossless commutation under the condition of ZVS because of

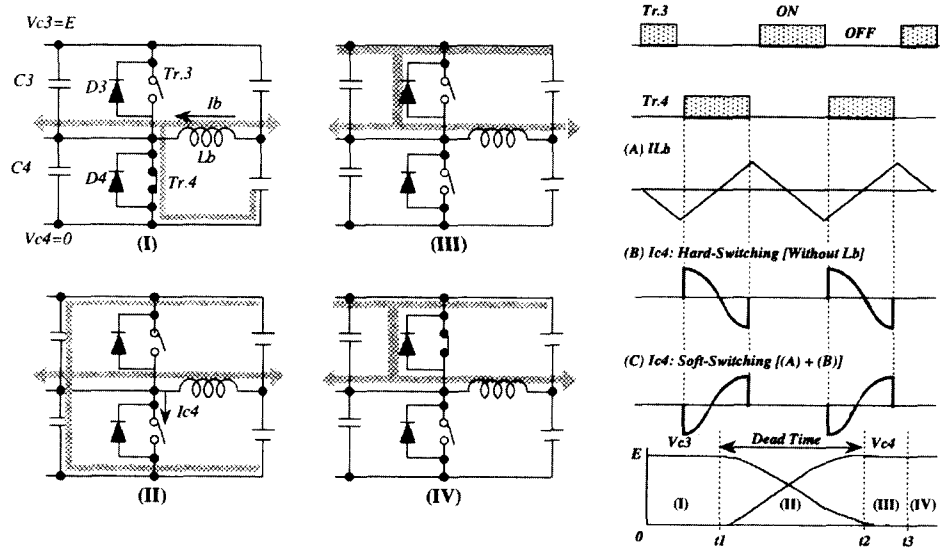


Fig. 6 Operation Principle of Soft-Switching Converter Using Resonant Poles

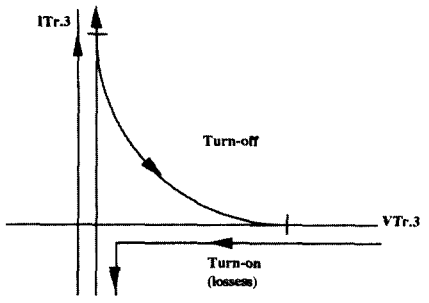


Fig. 7 Voltage-Current trajectory during Switching Commutations

voltage commutation due to lossless capacitive snubber effect.

The idealized current waveforms of the quasi-resonant inductor are shown in Fig. 6(a) and Fig. 6(b).

A typical waveform of the current flowing through $Q_4$ for hard-switching mode at turn-off in conventional PWM converter is also illustrated in this figure.

The current waveform of $Q_4$ for soft-switching PWM converter is shown in Fig. 6(c), which can be obtained by the addition of the current waveforms shown in Fig. 6(a) and (b).

Fig. 7 provides the switching state-variable trajectory on the current and voltage plane during capacitor voltage transition interval with a blanking time.

Because of this converter operation based upon the typical resonant-pole commutation, the considerable reductions in switching losses of main active power devices, high-power density, faster control performance as well as lowered EMI noise can be realized effectively under high-efficient operation even at HF switching.

## 6. Dynamical Circuit Modeling of System Components

It is indispensable to estimate the inherent parasitic circuit components included into the high-frequency high-voltage transformer with a large turn ratio.

The primary windings of two HV transformers are connected in parallel and its secondary windings are connected in series.

According to the frequency characteristics of HV transformer, the resonant phenomenon generates in the higher frequency range of 20kHz.

As a result, its lumped leakage inductance reduced into its primary side is measured and its lumped frequency stray capacitance reduced into the primary side are inherently observed when this specially-designed transformer is operated at a frequency of about 20kHz.

In addition to these, the energy dissipative circuit constants are included in the HV transformer, which are equivalent to a copper loss and an iron loss resistances $R_1$ and $R_2$.

Its parasitic lumped leakage inductance can be expressed as the circuit constant $L_t$ which is used as a series resonant inductor, when the transformer operates in the frequency range of 20kHz.

In addition, its stray capacitances which are distributively formed between the secondary winding layers of HV transformer can be expressed as the lumped parasitic capacitor circuit constant $C_t$, which is used as a parallel resonant capacitor.

The resistance $R_1$ inserted in series with the leakage inductance $L_t$ is equivalent to a total copper loss component existing in the transformer primary and secondary windings.

$R_2$ is connected in parallel with the primary terminals of the transformer is equivalent to its iron loss resistance component.

In this case, its magnetizing inductor $L_m$ is connected in parallel with $R_2$. The case that the transformer is operated at the HF of 20kHz, $L_m$ may be neglected as compared with $L_t$.

Two specially-designed HV transformers with ferrite core are exactly expressed by the equivalent dynamical circuit model.

This model is represented by parallel resonant tank composed of $L_t$ and $C_t$ reduced into its primary-side, energy dissipative constants $R_1$ and $R_2$ and an ideal transformer with an extremely large turn ratio.

On the other hand, the equivalent input capacitance $C_x$ of high-voltage DC cable is used as DC smoothing capacitor. This capacitance $C_x$ is reduced into its primary side. This smoothing capacitor is expressed as the circuit constant $C_c$ in its primary-side.

This smoothing capacitor is connected with a full-bridge diode rectifier, which is cascaded into the ideal isolated transformer with a unity turn ratio in its primary side.

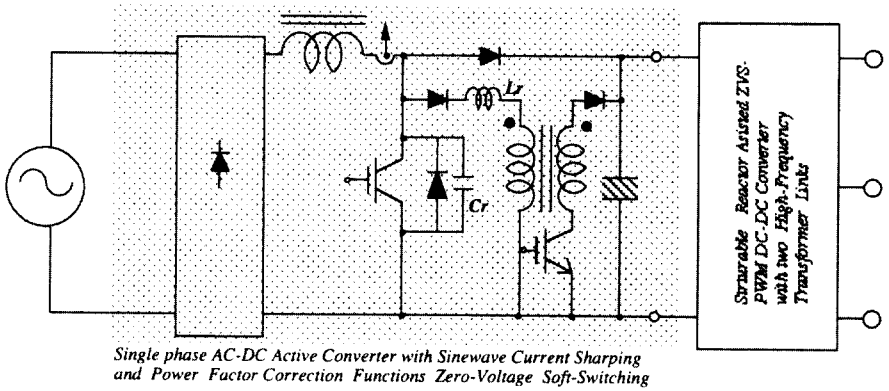


Fig. 8 New Low-noise ZVS-PWM Active Converter High-Frequency Inverter Cascade System for Heater Current Regulation

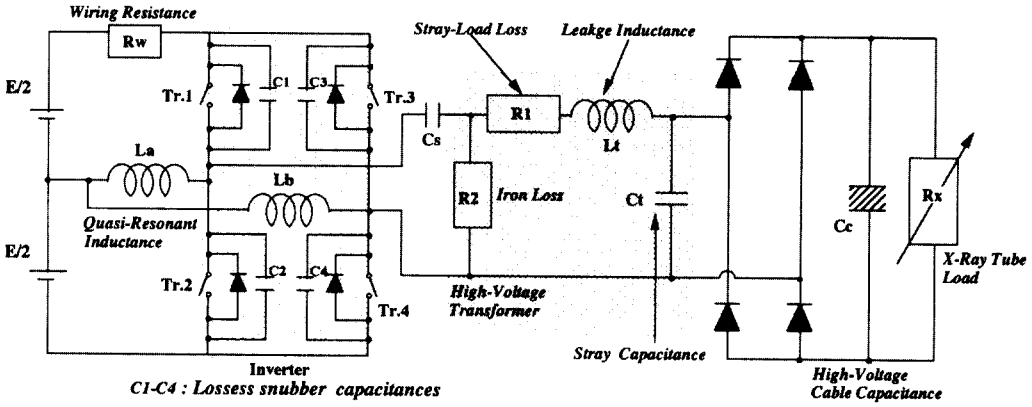


Fig. 9 Equivalent Circuit Model for Newly-developed PWM Converter with Two Resonant-poles

Moreover, the X-ray tube in both steady-state and dynamic operations can be represented by the resistance circuit load, which is adjusted in accordance with its heater current regulation.

The heater current with a low ripple is supplied through the latest quasi-resonant ZVS-PWM DC-DC converter with HF transformer link, which is connected to the X-ray filament resistance circuit.

The soft-switching power conversion circuit for heater current regulation is also shown in Fig. 8. As a result, the load resistance $R_x$ is widely adjusted in accordance with the heater current reference for some specified requirements. This pure resistance is reduced into the primary-side of high voltage transformer. This can be expressed as the circuit constant $R_x$. Considering the above various procedures, the whole equivalent dynamical circuit modeling of the newly-developed soft-switching PWM DC-DC converter with HFHV transformer for X-ray generating system is schematically shown in Fig. 9.

## 7. Resonant Pole assisted Converter Characteristics

### 7.1 Evaluations of Steady-State Operating Waveforms

Fig. 10 shows the voltage and current waveforms of the resonant pole-assisted multi-resonant ZVS-PWM inverter type DC-DC high-power converter operating at $\psi=30°$ and $\psi=90°$.

When the phase-shifted angle $\psi$ is changed the current waveforms flowing through the power switches $S_2$ and $S_4$ shown in Fig. 11.

Observing these switching current waveforms, it is

proved that $S_2$ and $S_4$ incorporated into the inverter arms can operate under the operating mechanism of ZVS in spite of phase-shifted PWM control processing from $\psi=0°$ to $\psi=180°$.

In particular, $S_1$ and $S_4$ operate at ZVS and ZCS hybrid switching modes when these switches turn on.

On the other hand, these switches turn off at ZVS mode for all the regulation ranges from $\psi=0$ to $\psi=\pi$ as well as wide load variation.

Zero-voltage soft switching transitions can be assuredly achieved at turn-on and turn-off.

### 7.2 Steady-State Voltage Regulation Characteristics

Fig. 12 illustrates the steady-state voltage regulation characteristics of this multi-resonant ZVS-PWM DC-DC converter with HFHV link.

These characteristics ($\psi$ vs. $V_o$ characteristics; $\psi$: $0<\psi<\pi$, $V_o$ : DC output voltage) are basically the same as single-resonant PWM DC-DC converter discussed output voltage can be regulated from 0 to maximum by means of adjusting $\psi$ as control variable.

However, the voltage control sensitivity of the converter becomes different according to $\psi$.

### 7.3 Converter Loss Analysis and Comparative Studies

The loss analysis obtained experimentally from the produced 50kW-120kV resonant pole-assisted multi-resonant ZVS-PWM converter with 20kHz HV transformer link which operates under the quasi- resonant principle of ZVS mode is illustrated in Fig. 13, as compared with the loss analysis for series and parallel resonant PWM DC-DC converter with the HV transformer link.

The switching losses of IGBTs incorporated into the multi-resonant ZVS-PWM inverter are considerably lowered under a heavy load and a light load conditions.

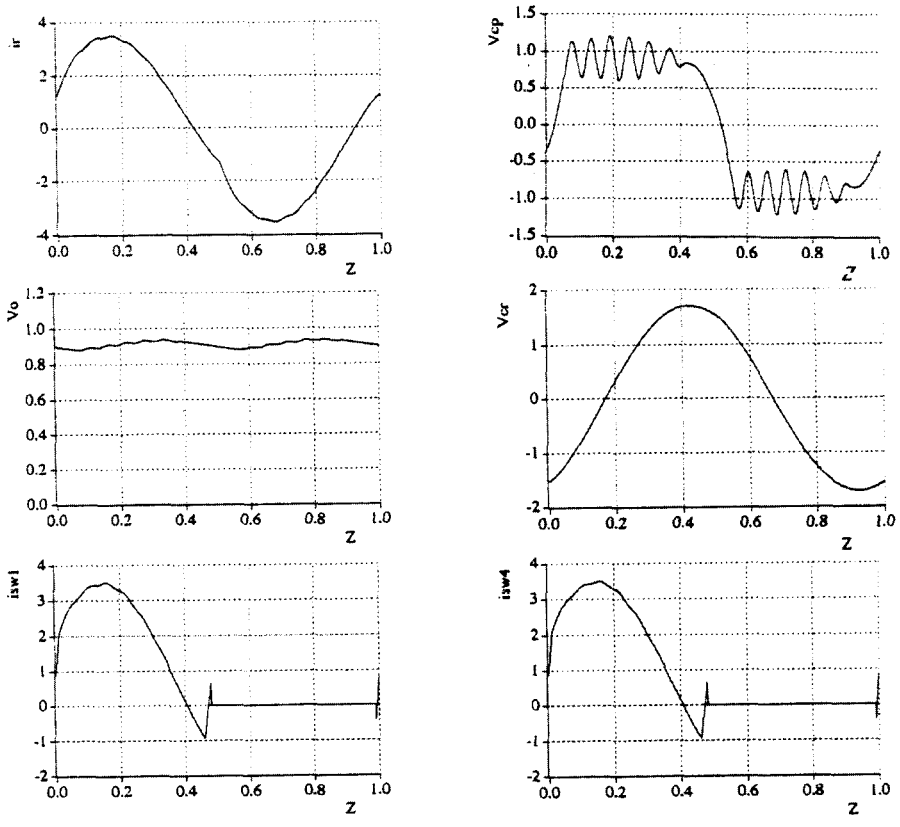


Fig. 10 Voltage and Current Waveformers of Resonant pole-assisted Multi-Resonant ZVS-PWM Inverter Type DC-DC Converter Operating $\phi=0$

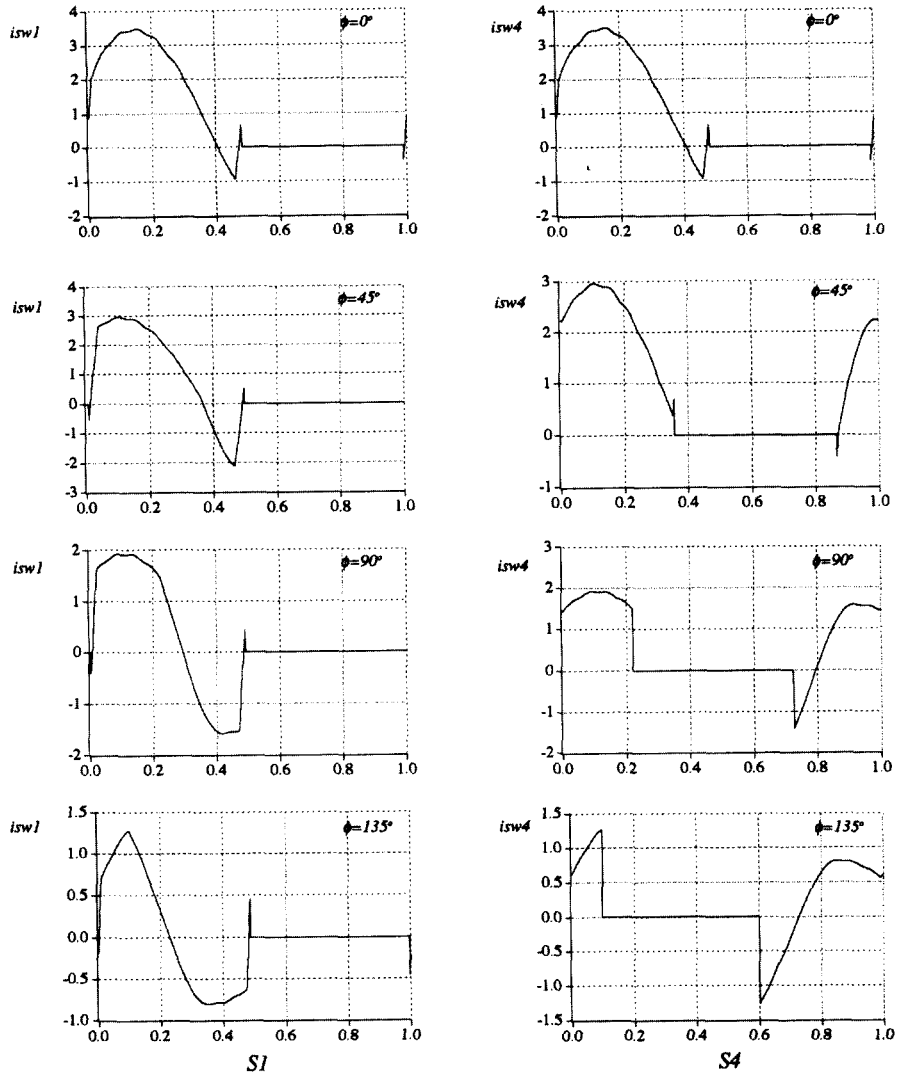


Fig. 11 Current Waveforms of S1 and S4 when Phase-Shifted Angle $\phi$ is changed

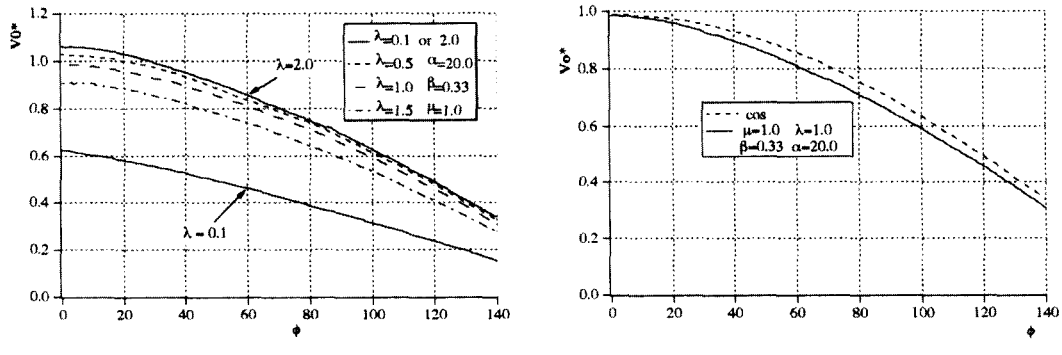


Fig. 12 Steady-state Voltage Regulation Charactersitics of the Multi-Resonant ZVS-PWM DC-DC Converter

In addition to this, substantial reduction in switching losses is performed in spite of a wide range of phase-shifted angle control processing and largely adjusted load resistance variations. In this case, the application-specific next generation IGBTs with an ultra lowered conduction voltage drop known as low frequency soft-switching family are required in order to decrease the conduction loss of IGBT.

The internal parasitic resistances $r_a$ and $r_b$ of quasi-resonant inductors $L_a$ and $L_b$ in the resonant pole circuits should be designed to be extremely lower in order to improve the converter efficiency under the light load conditions.

Fig.13 illustrates the comparative measured losses for the converter I shown in Fig. 1 and the converter shown in Fig. 2 under 50kW-120kV output ratings.

Fig. 14 is comparative measured waveforms for hard-switching and soft-switching converter under the output power of 48kW.

This converter using the latest IGBTs can be expected so as to be more efficient and acceptable for the high-power applications, if its operating frequency can be designed to be more elevated.

A HV transformer with a ferrite core structure should be designed so as to operate efficiently in the high frequency range higher than 20kHz in order to improve the performances in power conversion efficiency and control response and to minimize the physical size and weight as well as EMI noise generation.

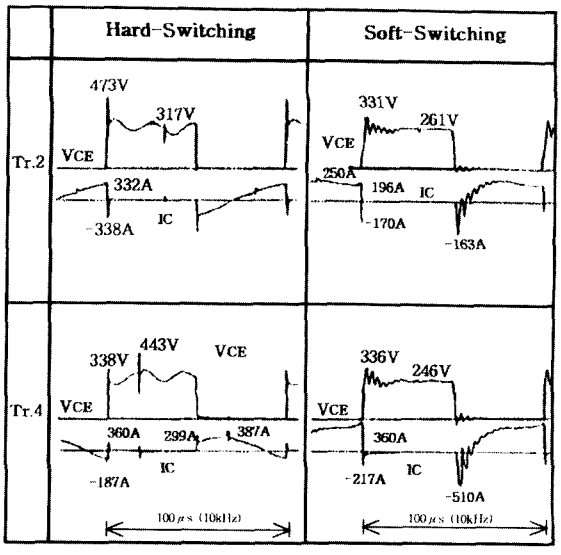


Fig. 14 Comparative measured waveforms for hard-switching and soft-switching converter under the output power of 48kW

## 8. Conclusions

A 50kW-120kV phase-shifted ZVS-PWM multi-resonant DC-DC high-power converter with two 20kHz HV transformers-coupled stage, which incorporates the series capacitor-connected transformer parasitic parallel resonant tank circuit into auxiliary quasi-resonant commutation poles, has been developed by way of trial for a high-power density power supply used in a diagnostic

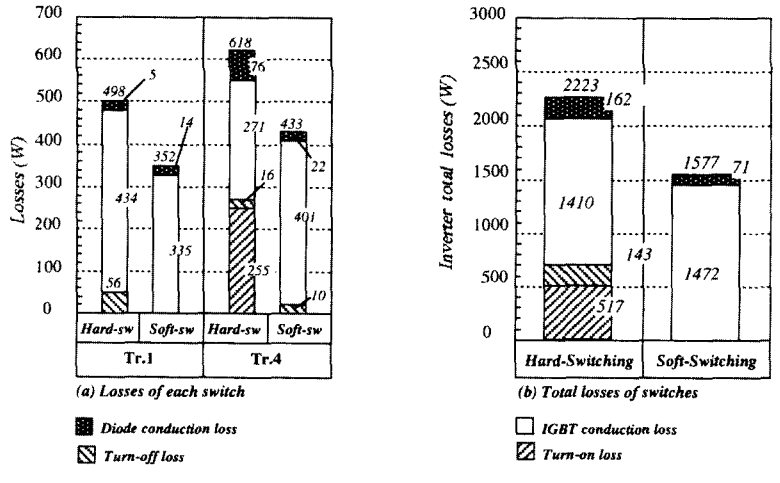


Fig. 13 Loss Analysis for Hard-Switching and Soft-Switching under the outpower:50KW

X-ray imaging system for medical power conditioner.

Its converter characteristics under a constant frequency PWM voltage regulation ranges and load variations have been illustrated on the basis of the computer-aided simulation analysis due to the circuit modeling of converter system components.

As compared with a previously-developed a constant frequency phase-shift PWM converter with a series and parallel resonant AC tank, it has been substantially proven that this converter topology results in considerable reductions in switching losses of IGBTs used, their lowered electrical dynamic voltage and current stresses as well as alleviated EMI noise level under the conditions of wide load setting values and PWM regulation process when largely-changed as well as when adjusted input voltage disturbances and periodic small voltage ripple fluctuations.

In the future, extended efficient quasi-resonant pole topologies operating at ZVS transition mode should be actively taken advantage of in place of a resonant-pole topology treated here.

The advanced resonant pole-assisted ZVS-PWM DC-DC converter version operating in the frequency range higher than 30kHz will have to be developed in order to provide the further improved performances for the X-ray high-power applications in medical and industrial usages, and the other distributed high power supply systems.

## References


[1] Y. Chorin, H. Foch and J. Salessens, "Study of Resonant Converter using Power Transistors in 25kW Power Supply", IEEE-PESC and ESA Proceedings, p. 295, June, 1985.

[2] M. Nakaoka, Y. J. Kim, and H. Ogiwara, "Modern Digitally-Controlled Constant High-Frequency PWM Resonant DC-DC Converter and Its new Practical Application", Proc. of IAS Conference, Vol. 1, pp. 1088~1097, Oct. 1991.

[3] Y. J. Kim, M.Nakaoka and S.Nagai, "The state-of-the art phase-shifted ZVS-PWM Series & Parallel Hybrid Resonant DC-DC Power Converter using Internal Parasitic Circuit Components and New Digital Control", IEEE-PESC Proc., Vol. 1, p. 62~70,June 1992.

[4] Y. J. Kim, S. Nagai and M. Nakaoka, "Phase-Shifted PWM Resonant Pole & Series-Parallel Resonant Tank DC-DC Converter with High-Voltage AC Transformer & DC Cable Link and Its Linearization Compensated Feedforward and feedback Control Scheme", CJPEC Conference Proc., Vol. I, pp, 42~49, Sept. 1992.

[5] Y. J. Kim, Y. Maruyama and M. Nakaoka, "Practical Evaluations of Resonant-Pole Assisted ZVS-PWM DC-DC Converter with Series Capacitor-Connected Transformer Parasitic Parallel Resonant Tank", IEEE-PESC Proc., pp, 795~802, June 1993

[6] Y. J. Kim and M. Nakaoka, "Comparative Characteristic Evaluations of Specially-Designed High-Voltage Transformer Parasitic Resonant PWM Inverter-Linked High-Power DC-DC Converter", IEEE-PESC Proceedings, pp. 120~127, June 1995


## 〈저 자 소 개〉


**Yong-Ju Kim**

Yong-Ju Kim was born in Korea on Mar. 19. 1960. He received the B.S. and M.S. degrees in Electrical Engineering from the Kon-Kuk University, Seoul, Korea, in 1984. and 1988, respectively, and the Dr. Eng. degree from Kobe University, Kobe, Japan, in 1996. He has been with the Sam-Sung Display Company in 1996. Since 1996 he has been a Patent Examiner, Semiconductor Examination Division I, Korean Industrial Property Office.

**Dae-Chul Shin**

Dae-Chul Shin was born in Korea on Mar, 2, 1952. He received the B · S. M · S, Ph · D degrees in Electrical Engineering from the Kon-KuK university, seoul, Korea, in 1973, 1975, 1991, respectively. Since 1979 he has been a professor of the Electrical Engineering of 1st Engineering Faculty, Hoseo University, Asan, Chung Nam, Korea. He was a visiting scholar in the Department of Electrical Engineering, Nagasagi university during 1989~1990.